Journal of Applied Polymer Science

Mechanical characterization of high-performance graphene oxide incorporated aligned fibroporous poly(carbonate urethane) membrane for potential biomedical applications

Sudhin Thampi,[1,2] Vignesh Muthuvijayan,[1] Ramesh Parameswaran[2]

[1]Department of Biotechnology, Bhupat and Jyoti Mehta School of Biosciences, Indian Institute of Technology Madras, Chennai 600036, India

[2]Polymer Processing Laboratory, Biomedical Technology Wing, Sree Chitra Thirunal Institute of Medical Sciences and Technology, Thiruvananthapuram 695012, India

Correspondence to: R. Parameswaran (E - mail: rameshsctimst@hotmail.com)

ABSTRACT: In this article, we report the development of graphene oxide (GO) reinforced electrospun poly(carbonate urethane) (PCU) nanocomposite membranes intended for biomedical applications. In this study, we aimed to improve the mechanical properties of PCU fibroporous electrospun membranes through fiber alignment and GO incorporation. Membranes with 1, 1.5, and 3% loadings of GO were evaluated for their morphology, mechanical properties, crystallinity, biocompatibility, and hemocompatibility. The mechanical properties were assessed under both static and dynamic conditions to explore the tensile characteristics and viscoelastic properties. The results show that GO presented a good dispersion and exfoliation in the PCU matrix, contributing to an increase in the mechanical performance. The static mechanical properties indicated a 55% increase in the tensile strength, a 127% increase in toughness for 1.5 wt % GO loading and the achievement of a maximum strength reinforcement efficiency value at the same loading. Crystallinity changes in membranes were examined by X-ray diffraction analysis. *In vitro* cytotoxicity tests with L-929 fibroblast cells and percentage hemolysis tests with fresh venous blood displayed the membranes to be cytocompatible with acceptable levels of hemolytic characteristics. Accordingly, these results highlight the potential of this mechanically improved composite membrane's application in the biomedical field. © 2015 Wiley Periodicals, Inc. J. Appl. Polym. Sci. **2015**, *132*, 41809.

KEYWORDS: biomedical applications; composites; electrospinning; mechanical properties; membranes

Received 19 September 2014; accepted 23 November 2014

DOI: 10.1002/app.41809

INTRODUCTION

Polymer nanocomposites have recently displayed considerable interest because of their cost-effective processability, light weight and tunable physicomechanical properties.[1] The field of polymeric nanocomposites has evolved significantly over the last decade. Graphene (G) and G-based materials have attracted intensive research interest because of their inherent properties, such as their excellent mechanical strength, high electrical conductivity, and outstanding thermal resistance.[2] Deriving from the different composition, size and morphology, versatile and unique properties are expected when they are combined with specific polymers.[3] Melt compounding/extrusion techniques are the most common methods for making polymer-based composites. However, the importance of the solution exfoliation of graphene oxide (GO) has demonstrated the processability of these candidates into polymer nanocomposites, transparent conducting films, and drug-delivery vehicles.[3] To date, much of the solution processing of GO has been carried out by simple sonication in water.[4] The preparation of large-scale GO dispersions in organic solvents is also highly desirable and may further broaden the scope of applications and facilitate the practical use of G-based materials. Park *et al.*[5] reported the achievement of colloidal suspensions of highly reduced graphene oxide (rGO) in various organic solvents by the dilution of a colloidal suspension of rGO platelets in dimethylformamide (DMF):water (9:1) and also with solvents, such as DMF, *N*-methyl pyrrolidone, ethanol, acetonitrile and dimethyl sulfoxide.

Segmented polyurethanes (PUs) have been used in the biomedical field for over 5 decades. The versatility of this polymeric family is due to its useful properties, such as its good mechanical strength, ease of handling and hemocompatibility.[6] However, biomedical applications including implantation in humans, currently appear limited because of their adverse effects, such as hydrolytic, oxidative and enzymatic degradation as the body

environment is rather an aggressive medium.[7] Poly (carbonate urethane)s (PCUs) represent a new class of biostable PUs with superior biocompatibility, physical properties and biostability.[8] They are used in a wide range of biomedical applications such as heart valves,[9] membranes[10] and vascular prosthesis.[11] The incorporation of G or rGO into PUs is still being explored for improving the various properties of PUs. Kim *et al.*[12] compared carbon sheets exfoliated from graphite oxide via chemical modifications with isocyanate-treated GO and thermal exfoliation [thermally reduced graphene oxide (TRG)]. Incorporation of as low as 0.5 wt % TRG produced electrically conductive thermoplastic PU, whereas 3 wt % isocyanate-treated GO led to a 10-fold increase in the tensile stiffness.

Electrospinning of polymers is a versatile technique for the preparation of ultrafine, continuous submicrometer and/or nanofibers. In the biomedical field, the technique of electrospinning is used for several applications, including filtration and protective materials, electrical and optical applications, sensors, nanofiber-reinforced composites and so on.[12] Recently, many research groups have reported the incorporation of GO into polymers by electrospinning to obtain a fibroporous membrane. Fibroporous polymeric composite membranes from polymers such as poly(vinyl alcohol)[13] and poly(ε-caprolactone)[14] prepared by electrospinning have shown superior mechanical, thermal and biological properties. Although a lot of references appeared on electrospun nanocomposites, not much research work has been done on electrospun GO-incorporated PCU membranes.

The purpose of this study was to understand the effects of GO incorporation onto the PCU electrospun membrane's physicomechanical properties and thus to explore the potential of this modified membrane for biomedical applications. The membrane was subjected to morphological and thermomechanical analysis to evaluate the dispersion of GO and the viscoelastic nature of the membrane. The biological reaction to the culture of the fibroblast cells on the membrane and hemolytic property for blood-contact applications was also assessed.

EXPERIMENTAL

Materials

PCU, with the trade name of Carbothane manufactured by Lubrizol Corp., was used in this study. PCU was dissolved in mixture of DMF and tetrahydrofuran (THF; 50/50 v/v) at a total concentration of 12% (w/v %) for electrospinning. Graphite flakes was procured from Sigma-Aldrich. DMF, THF, H_2SO_4, H_3PO_4, $KMnO_4$, HCl and 30% H_2O_2 were purchased from Merck (India). A 3-(4,5-dimethylthiazol-2-yl)-2,5-diphenyltetrazolium bromide (MTT; a tetrazolium salt) assay kit was purchased from Hi Media (India). Deionized water was used throughout this study.

Methods

Electrospinning of PCU (Carbothane). A syringe with a PCU solution was loaded onto the electrospinning unit. The syringe was capped with a 21-gauge blunt-end needle (spinneret), and a positive potential was connected at the needle end with a power supply (Γ high voltage), whereas the negative potential was connected to the target. A stationary plate and a rotating mandrel at 2500 rpm kept at a distance of 16 cm were used as targets to obtain poly(carbonate urethane) random fibers (PCURF) and poly(carbonate urethane) aligned fibers (PCUAF), respectively. The PCU solution was delivered to the charged spinneret by the syringe pump at a flow rate of 1 mL/h and electrospun at 8–10 kV potential. The process was carried out at ambient temperature (28 ± 2°C).

Synthesis of GO and the Electrospinning of the Nanocomposite. GO was prepared via an improved Hummers method given by Marcano *et al.*[15] The composite solutions were prepared by tip sonication of GO at weight percentages of 1 wt % (PCU/1% GO), 1.5 wt % (PCU/1.5% GO), and 3 wt % (PCU/3% GO) of PCU. Sonication was done for 45 min to exfoliate and disperse the solutions in DMF and THF (1:1) mixtures followed by the overnight stirring with PCU pellets. Electrospinning was done onto a rotating mandrel under similar conditions but at various voltages of 14–15, 16–17, and 17–19 kV for 1, 1.5, and 3% GO loadings, respectively. The electrospun sheets were retrieved from the mandrel and air-dried to remove any residual solvent.

Morphological Analysis [Scanning Electron Microscopy (SEM)]. SEM (Hitachi model S-2400) was used to study the morphology and average diameter of the fibers. Sample preparation was done by the sputtering of thin, flat sections of the materials with gold–palladium. The reported data on the average fiber diameter are the means of 25 measurements at different areas with Image J software.

Mechanical Analysis. The sheets were cut along the direction of fiber alignment into dumbbell specimens for tensile testing and rectangular pieces for dynamic mechanical analysis (DMA) testing. Tensile testing was performed with an Instron 3345 model equipped with a load cell of 100 N, following ASTM D 638. Standard dumbbell-shaped specimens were cut with an ISO 527-2 type 5A die and tested at 25 ± 2°C at a crosshead speed of 100.0 mm/min, with sample thicknesses that varied from 0.2 to 0.3 mm (sample size $n = 5$). The stress and strain calculation was done manually from the load and extension data that we acquired. The tensile strength was taken from the highest stress value achieved, whereas the toughness was the area under the stress–strain curve.

DMA was done in tensile mode with a Tritec 2000B DMA instrument (Triton Technology, Ltd., United Kingdom) on a rectangular sample of 4-mm width, 20-mm length and 0.2-mm thickness. A frequency of 1 Hz with an amplitude of dynamic deformation of 50 μm was applied in the temperature-ramp experiments. Thermal cycling was monitored within −100 to 60°C at a heating rate of 1°C/min.

Statistical Analysis. The tensile strength data for the three classes, that is, PCURF, PCUAF, and PCU/GO, membranes were analyzed statistically with an analysis of variance one-way test, and p values were obtained to weigh the significance of the experiment designed. Significance was assigned at p values of less than 0.05.

Strength-Reinforcing Efficiency (ε). The ε value of the GO nanoplatelets was evaluated in the thermoplastic PCU fibroporous matrix. It was carried out with the rule of mixtures [eq. (1)]:[16]

$$Y_c = \varepsilon Y_f \varphi + Y_m(1-\varphi) \quad (1)$$

where Y_c, Y_f, and Y_m are the mechanical properties (tensile strengths) of the composite, filler and matrix, respectively, and φ is the volume fraction. This parameter represents the efficiency of the filler as a reinforcing phase and is a good measure for comparing composite systems having similar fillers.

Exfoliation and Intercalation Analysis with X-ray diffraction (XRD). XRD data were collected with a Bruker D8 Advance diffractometer with Cu Kα radiation at a scan speed of 4°/min over 5–50°. The GO sample was analyzed in powder form, whereas for electrospun PCU and PCU/GO composite membranes, a 20-mm diameter disc were used.

***In Vitro* Cytotoxicity Test.** An *in vitro* cytotoxicity test was performed with a direct contact method as per ISO 10993-5. The material was sterilized by dipping in ethanol for an hour followed by phosphate buffer saline (PBS) washing and overnight drying. It was further UV-treated for 10 min just before the experiment. The culture medium from the L-929 mouse fibroblast cells monolayer was replaced with fresh medium. The test samples, negative controls and positive controls in triplicate were placed on the cells. After incubation at 37 ± 1°C for 24–26 h, the cell monolayer was examined microscopically for response around the test samples. The reactivity was graded on the basis of the zone of lysis, vacuolization, detachment, and membrane disintegration.

The MTT assay was performed to measure the metabolic activity of cells to reduce yellow-colored MTT to purple-colored formazan. The material extract was prepared by the incubation of disc-shaped test material with a diameter of 3 mm in high-glucose Dulbecco's modified eagle's medium culture medium supplemented with 10% fetal bovine serum, 1× antibiotic–antimycotic solution, and 0.37% sodium bicarbonate at 37 ± 1°C for 24 ± 2 h. The extract (100%) was diluted to 50% (1:1) and 25% (1:4) with culture medium. Cells cultured in normal medium without any extract was considered as a cell control. The control and test sample extracts were added to a subconfluent monolayer of L-929 cells in triplicate and incubated at 37 ± 1°C for 24 ± 2 h. Later, a stock MTT solution (20 μL of 5 mg/mL PBS) was added to the extract and control medium; incubated with protection from light for 4 h. After 4 h of incubation, 200 μL of dimethyl sulfoxide was added to the wells and the plates were put in an orbital shaker (GeNei, SLM-INC-OS-250, India) to dissolve the formazan crystals. The plate was quantified by the measurement of the absorbance at 570 nm with an ultraviolet–visible microplate reader and the percentage viability of the cells was calculated. The reported data were the means and standard deviations (SDs) of three parallel runs for each sample.

Hemolysis Assay. The hemolytic character of the material was assessed by means of an *in vitro* hemolysis test. Fresh venous blood was collected from a volunteer in anticoagulant citrate phosphate dextrose adenine (CPD-A) tubes and care was taken to prevent mechanical hemolysis. Total hemoglobin (Hb) was analyzed with a hematology analyzer (Sysmex-K4500). Disc-shape test material of 4 mm diameter in triplicate was immersed in PBS for 5 min before exposure to blood. The samples were kept in a polystyrene plate; 2 mL of blood was added to each well, and a well without any sample was treated as a reference (REF). A volume of 1 mL of blood was taken immediately for initial analysis and the remaining 1 mL of blood was incubated with a sample for 30 min under agitation at 70 ± 5 rpm at 35 ± 2°C.

The blood samples were centrifuged at 4000 rpm for 15 min; the platelet poor plasma was carefully removed and diluted 1:30 in 0.1% Na_2CO_3. The free hemoglobin (fHb) liberated into the plasma after exposure to samples was measured with a UV spectrophotometer (Shimadzu UV-1800) as per eq. (2):[17]

$$\text{fHb} = 1.65A_{415} - 0.93A_{380} - 0.73A_{450} \quad (2)$$

where A_{415}, A_{380}, and A_{450} are the absorbances at 415, 380, and 450 nm wavelengths, respectively. The percentage hemolysis was calculated with the formula (fHb/Total Hb) × 100. The hemolysis was thus calculated, and the results are expressed as the mean plus or minus SD ($n = 3$).

RESULTS AND DISCUSSION

Morphological Analysis by SEM

Electrospun fibers are generally collected as nonwoven or randomly arranged structures because of the whipping instability of the electrospun jet. A high-speed rotating drum has been recognized as the simplest procedure for obtaining highly aligned microfibers/nanofibers.[18] In our system, highly aligned fibroporous membranes of PCU and PCU/GO were obtained at 2500 rpm. Figure 1(a,b) shows the SEM images of the PCURF and PCUAF electrospun at 8–10 kV with respective fiber diameters of about 939 ± 195 and 598 ± 58 nm. This thinning effect was observed in electrospinning systems, where a rotating target with a high surface velocity was used.[19] Figure 1(c-e) shows the aligned PCU/GO membranes with various concentrations of GO. A 1% GO displayed an average fiber diameter of 390 ± 96 nm, and as the concentration of GO was increased from 1 to 3%, the fiber diameter increased to 444 ± 102 nm. There was a decrease in the fiber diameter from 598 ± 58 nm for PCUAF to 390 ± 96 nm after the incorporation of 1% GO; this may have been due to the increased voltage of electrospinning needed to adjust the increased viscosity of the solution. Subsequently, as the concentration of GO increased, the viscosity of the spinning solution also increased and so increased the fiber diameter.[20]

Tensile Properties

The mechanical properties, in terms of the tensile strength and toughness, are summarized in Table I. The tensile strength of the PCURF membrane was about 11.6 MPa, whereas that of the PCUAF membrane was 23.04 MPa. This increase in the tensile strength may have been due to the reduction in the fiber diameter, which led to a closer packing of fibers in the membranes.

The effects of the introduction of 1, 1.5, and 3 wt % GO on the tensile properties of PCUAF were analyzed. Table I provides the tensile properties of the membrane and the stress–strain curve is given in Figure 2. At particular strain values, the

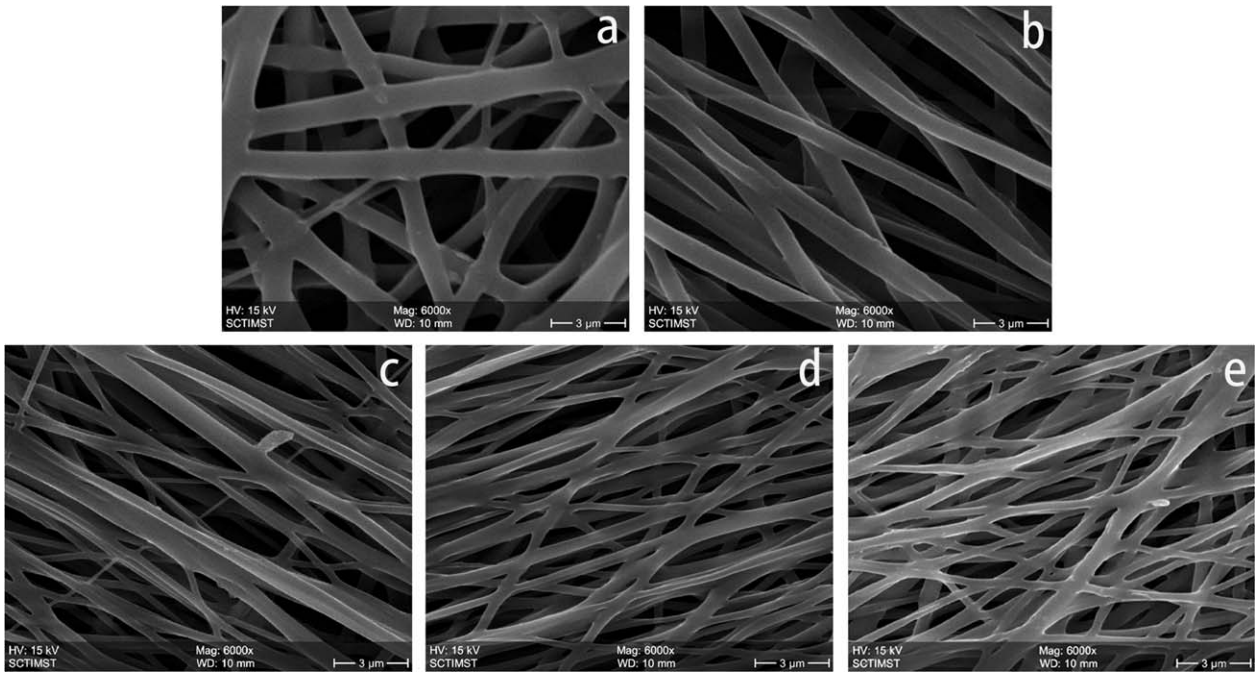

Figure 1. SEM micrographs of the PCU electrospun membranes (DMF/THF mixed solvent at 1 mL/h): (a) PCURF (8–10 kV), (b) PCUAF (8–10 kV), (c) PCU/1% GO (14–15 kV), (d) PCU/1.5% GO (16–17 kV) and (e) PCU/3% GO (17–19 kV).

strengthening of the membrane was observed; this may have been due to the strain-induced crystallization of the polymer membrane and resulted in strain hardening. This phenomenon was observed to become more prominent as the fibers became aligned in PCUAF and also by GO incorporation in the composite membranes.[21] After the incorporation of 1% GO, the tensile strength increased from 23.04 to 28.6 MPa; this was further increased to 35.6 MPa with the incorporation of 1.5% GO. However, at 3% GO, there was a reduction in the tensile strength; this indicated that a 1.5% loading could have been the optimum filler loading. With the increase in tensile strength, the toughness also increased from 6.1 to 13.89 MPa; this may have been due to strain hardening, wherein the orientation of the polymer molecules and the filler content forced the stress to distribute over a greater surface area.[22]

The improvement in the tensile properties may have been due to the fact that the applied load was transmitted from the matrix to the GO platelets at the interface in the GO-reinforced composites. Thus, the aligned composite fibers showed an efficient load-carrying capacity because of the better interface between the polymer and nanoplatelets.

The mechanical strength experiment design for randomness, alignment, and further incorporation of 1, 1.5, and 3% GO were of statistical significance ($n = 5$, $p < 0.05$); this indicated that the alignment of fibers and GO reinforcement obviously contributed to the improvement of the tensile strength.

Reinforcing Efficiency of the GO Nanoplatelets. The reinforcing efficiency calculation, although a simple technique, provides an insightful comparison of the filler–polymer interphase.[23] Various methods were designed to incorporate G or GO-based fillers in PU-based thermoplastic elastomers. Yousefi *et al.*[24] compared ε values for various incorporation techniques for the PU matrices, and the latex blending technique showed superior ε values.

ε was calculated for the electrospun composite membranes on similar lines (Table I). The reported ε value was 112×10^{-4} (with the latex blending method) for 3 wt % GO loading,[24] whereas we obtained a value of 142×10^{-4} with the electrospun method at a lower loading (1.5 wt %). These results confirm that electrospinning technique gave a much better strength-reinforcing efficacy for this elastomeric matrix.

Table I. Average Fiber Diameters, Tensile Properties, and ε of the PCU and Composite Electrospun Membranes

Sample	Average fiber diameter (nm)	Tensile strength (MPa)	Toughness (MPa)	ε ($\times 10^{-4}$)
PCURF	939 ± 195	11.67 ± 0.73	11.03 ± 0.4	—
PCUAF	597 ± 58	23.04 ± 0.94	6.1 ± 0.7	—
PCU/1% GO	390 ± 96	28.6 ± 1.3	9.94 ± 0.8	95.45729
PCU/1.5% GO	409 ± 107	35.6 ± 1.1	13.89 ± 0.9	142.8614
PCU/3% GO	444 ± 102	30.6 ± 1.2	8.5 ± 1.08	44.23385

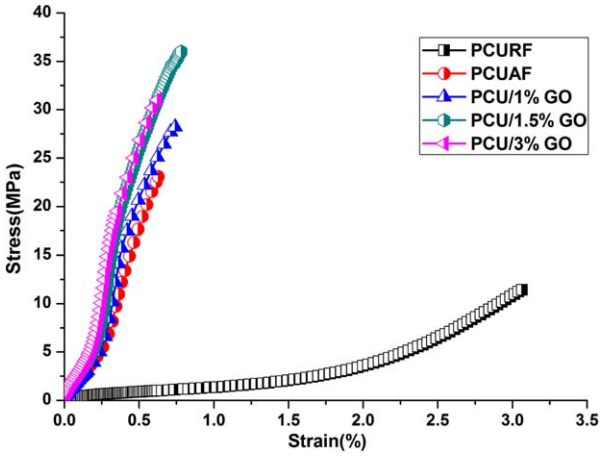

Figure 2. Stress–strain curves for the PCU and PCU/GO composite electrospun membranes. [Color figure can be viewed in the online issue, which is available at wileyonlinelibrary.com.]

DMA

DMA was carried out to study the thermomechanical properties of the composite electrospun membranes. Figure 3 shows the variation of tan δ with increasing temperature. The height of the tan δ peak is related to the amount of amorphous material present and the balance between the elastic and viscous phases of the materials.[25] The narrow tan δ peak, that is, the glass-transition temperature (T_g), for PCURF appeared at -7.8°C, whereas it widened and shifted for PCUAF to 21°C. This may have been due to fiber alignment and the closer packing of the nanofibers, which led to stiffer membranes. In the case of PCUs, as the filler content increased, the peak height of the tan δ curve decreased, and this restricted the degree of molecular mobility, and the peak widened because of the crystallinity.[26] As shown in Figure 3, the peak height of the composite nanofibrous membrane also decreased; this may have indicated an increase in GO's interaction with the harder segment in the PCU system. Several groups, such as hydroxyl, carboxyl, carbonyl, and epoxy groups, on the GO surface made this interface more interactive, and the gap between the layers allowed better

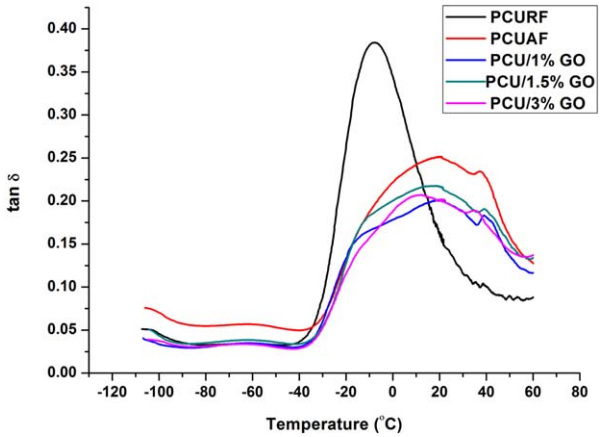

Figure 3. Temperature dependence of tan δ for the PCU and PCU/GO composite electrospun membranes. [Color figure can be viewed in the online issue, which is available at wileyonlinelibrary.com.]

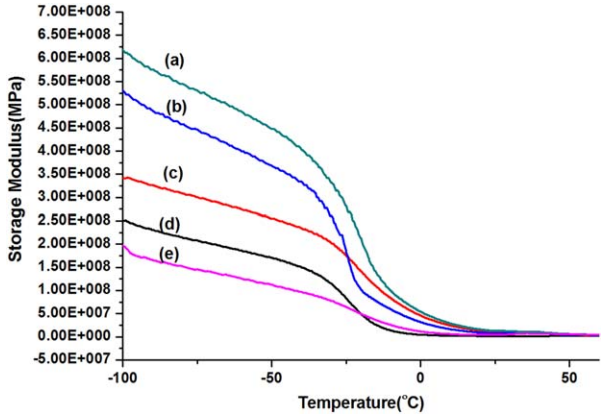

Figure 4. Temperature dependence of E' for the (a) PCU/1.5% GO, (b) PCU/1% GO, (c) PCUAF, (d) PCURF and (e) PCU/3% GO electrospun membranes. [Color figure can be viewed in the online issue, which is available at wileyonlinelibrary.com.]

intercalation with the polymer. The addition of GO thus led to a decrease in the tan δ peak maxima value with no significant shift in its peak position for PCU/1% GO and PCU/1.5% GO; this indicated lower damping characteristics.

For PCU/3% GO, there was a decrease in the peak maxima height and also a negative shift in the tan δ peak position to 10.8°C. This may have been due to a lesser matrix by volume to dissipate the vibrational energy and to the further agglomeration of GO nanoplatelets.

The variation in the storage modulus (E') with temperature is given in Figure 4. The E' values of all of the membranes decreased with increasing temperature. We noticed that E' increased with fiber alignment, and the further incorporation of GO as filler led to higher values prominently in the glassy state below T_g. We observed that in the glassy region, the modulus values gradually increased, whereas in the rubbery region, there was not much change. In the glassy region, the components were in a frozen state; this rendered it immobile, and hence, a high modulus was found. In case of the rubbery state as the temperature increased, the molecular components were in a highly mobile state and thus, showed no significant change in the modulus.[27]

E' showed its highest modulus for PCU/1.5% GO and significantly fell to its lowest value for PCU/3% GO composite as per the data provided at -50°C in Table II. The incorporation of 1% GO and 1.5% GO increased the value of E'; this may have

Table II. DMA Data, Including T_g Values, E', Values at -50°C, and Peak E'' Values, for the PCU and Composite Electrospun Membranes

Sample	T_g from tan δ peak maxima (°C)	E' at -50°C ($\times 10^2$ MPa)	Peak E'' (MPa)
PCURF	−7.8	1.70607	14.2
PCUAF	21.0	2.54461	18.7
PCU/1% GO	19.0	3.69318	18.5
PCU/1.5% GO	20.1	4.49695	27.4
PCU/3% GO	10.8	1.12034	5.7

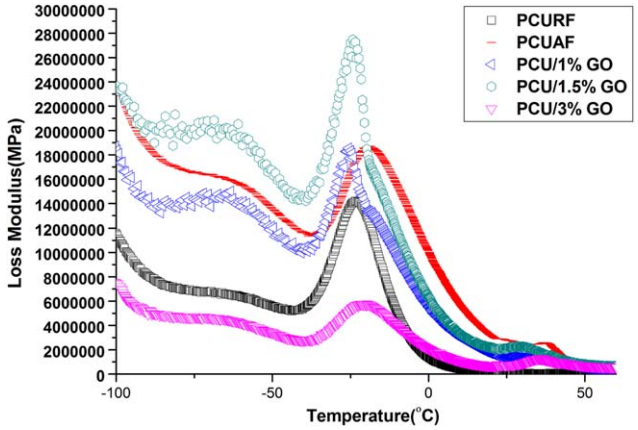

Figure 5. Temperature dependence of E'' for the PCU and GO composite electrospun membranes. [Color figure can be viewed in the online issue, which is available at wileyonlinelibrary.com.]

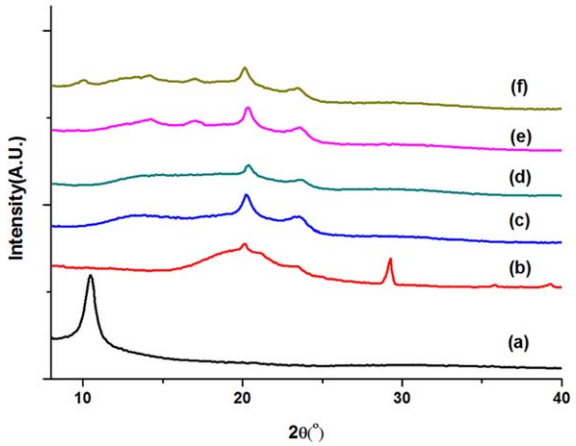

Figure 6. XRD pattern of the (a) GO, (b) PCURF, (c) PCUAF, (d) PCU/1% GO, (e) PCU/1.5% GO and (f) PCU/3% GO electrospun membranes. [Color figure can be viewed in the online issue, which is available at wileyonlinelibrary.com.]

been due to an increase in the capacity of the polymer matrix to support mechanical constraints with recoverable deformation. In particular, the composite stiffness increased substantially because of the stronger intermolecular interaction. The addition of GO thus allowed greater stress transfer at the interface and hence raised E'. To comply with biomedical applications, E' was also measured at 37°C for 1.5% loading and was found to be 10 GPa, whereas for PCURF, it was 0.6 GPa. This indicated the superior E' capability of the PCU/1.5% GO membrane.

The loss modulus (E'') is a measure of the energy dissipated as heat per cycle under the deformation experienced in a viscoelastic material. As shown in Figure 5, a narrowing of the peak was observed in E'' of the composite membranes PCU/1% GO and PCU/1.5% GO. This may have been an indication of a very good interphase between the filler and matrix that acted as if they were in the same physical state. The broadening of the peak may have been due to more free volume available at 3% loading.[25] The E'' peak value increased with GO nanoplatelet addition; at a 1.5% loading, E'' was found to be the highest, whereas the 3% loading drastically reduced the modulus value and was found to be lowest in the group of the electrospun membranes under study.

XRD

XRD is an efficient analytical technique for characterizing the intercalation and exfoliation in composites composed of polymer and layered materials.[28] The sharp peak at 2θ of 10.4° for GO indicated the effective oxidation of graphite with a interplanar spacings (d) value of 8.4Å and resulted in an increase in the interlayer distance between the G planes.

Characteristic XRD spectra of the membranes are shown in Figure 6. The spectrum of PCUAF showed sharper peaks in comparison to the broader ones of PCURF; this may have been due to the improved molecular alignment. The peaks at 13.94, 20.21 and 23.49°confirmed the presence of crystallinity due to aliphatic polyol in the carbothane. The broad peak at 13° was assigned to the internal structure of polycarbonate chains, namely, to the average distance of the carbonate groups, whereas the other peaks correspond to the crystalline domain.[29] The intercalation of GO with the polymer was shown by the appearance of a shifted peak at 14.2° and a new peak at 17.03° in 1.5%PCU/GO. In the case of the PCU/3% GO composite membrane, the characteristic GO peak also appeared; this may have been due to some amount of aggregation because of the increased content of the filler.

In Vitro Cytotoxicity

The process of electrospinning uses organic solvents that are toxic. Thus, it was a prerequisite for conducting *in vitro* cytocompatibility tests of these membranes before any biomedical applications.

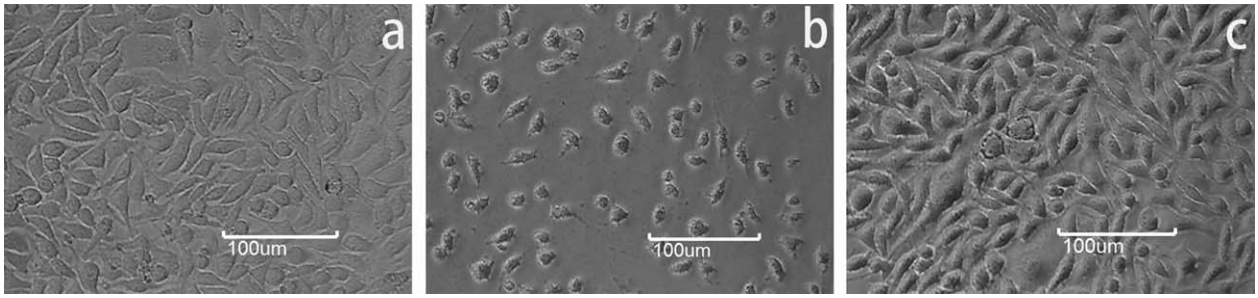

Figure 7. Cell morphology after a direct contact test: (a) negative control, (b) positive control and (c) PCU/GO composite electrospun membrane.

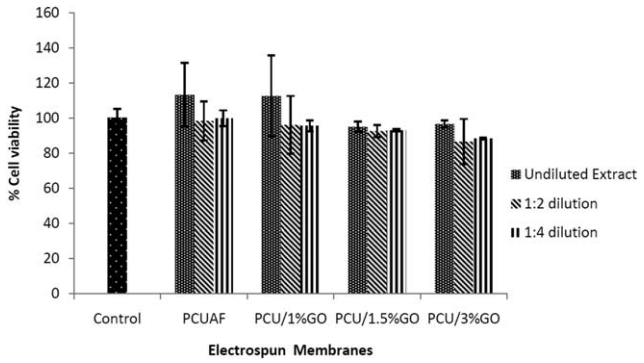

Figure 8. MTT assay representing the cell viability (%) of the L-929 fibroblast cells on electrospun membranes.

The fibroporous composite membranes were exposed directly to L-929 mouse fibroblast cells (Figure 7) for direct-contact tests, and the cells retained their spindle-shaped morphology and showed complete cytocompatibility.

An MTT assay was used to quantify the percentage cell viability of the electrospun membranes. Figure 8 shows the comparative cell viability percentage for each of the electrospun polymer and the polymer composite matrix. Previous works on PCURF have reported it to be cytocompatible,[30] and similar results have followed for PCUAF with good cell viability, whereas minimum cell viability was observed for PCU/3% GO composite membrane. Thus, electrospun composite membranes with improved mechanical properties showed a cytocompatible nature.

Hemolysis Assay

A hemolysis assay indicates the percentage hemolysis or quantifies the disruption to the membrane of red blood cells during the period of blood contact with implanted material. The disruption of a red blood cell membrane can cause its content to be released into the blood stream and this is not desired in the case of an implantable biomaterial. Figure 9 shows the hemolysis percentage for all of the electrospun polymeric and composite membranes. The results obtained supported the fact that the hemolysis percentage for the fibroporous membranes developed fell within an acceptable range[31] of less than 5%, as per the recommendation provided in ISO 10993-4; this indicated antihemolysis characteristics among all of the PCU and PCU/GO membranes.

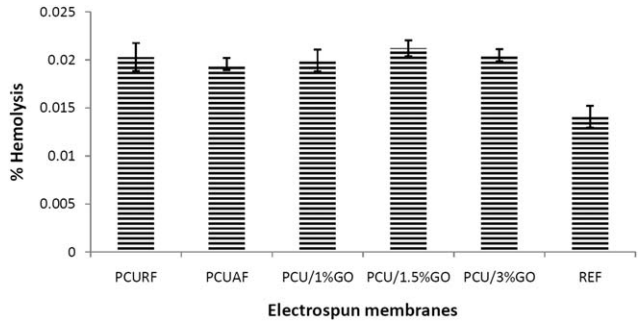

Figure 9. Graphical representation of the percentage of hemolysis of the PCURF, PCUAF, and composite electrospun membranes with 1, 1.5 and 3% loadings of GO.

CONCLUSIONS

Mechanically robust aligned hybrid fibers consisting of GO nanoplatelets embedded in a PCU matrix were prepared. SEM micrographs revealed a fibrous morphology with no bead formation; this indicated the good dispersion of GO in the PCU/GO composite. Tensile studies indicated the phenomenon of strain hardening and the electrospinning technique that we used was found to be better than the other fabrication techniques for the PU/GO composites. When compared to PCURF, PCUAF showed an improvement in the tensile strength by 97%. The tensile properties indicated a 55% increase in the tensile strength and a 127% increase in the toughness value for PCU/1.5% GO. However, for the PCU/3% GO membrane, there were decreases in the tensile strength and toughness; this indicated that 1.5% was the optimum concentration in this study. The DMA studies also indicated a similar trend, with a 30°C shift in T_g and better damping and E' characteristics for PCUAF and PCU/1.5% GO, whereas PCU/3% GO showed a decline in these properties. XRD analysis displayed improved crystallinity for PCU/1.5% GO when compared to the PCU/3% GO composite membranes. The composite membranes also displayed the cytocompatible nature of the L-929 fibroblast cells with permissible hemolytic characteristics for blood-contact applications. Further biological studies of this fibroporous composite membrane are required to access its efficacy for various potential biomedical applications.

ACKNOWLEDGMENTS

This study was performed at the Sree Chitra Thirunal Institute of Medical Sciences and Technology in collaboration with the Indian Institute of Technology Madras. One of the authors (S.T.) acknowledges the Indian Institute of Technology Madras for a fellowship and the Sree Chitra Thirunal Institute of Medical Sciences and Technology for the facility provided to perform this study.

REFERENCES

1. Jordan, J.; Jacob, K. I.; Tannenbaum, R.; Sharaf, M. A.; Jasiuk, I. *Mater. Sci. Eng. A* **2005**, *393*, 1.
2. Kuilla, T.; Bhadra, S.; Yao, D.; Kim, N. H.; Bose, S.; Lee, J. H. *Prog. Polym. Sci.* **2010**, *35*, 1350.
3. Huang, X.; Qi, X.; Boey, F.; Zhang, H. *Chem. Soc. Rev.* **2012**, *41*, 666.
4. Kim, J.; Cote, L. J.; Kim, F.; Yuan, W.; Shull, K. R.; Huang, J. *J. Am. Chem. Soc.* **2010**, *132*, 8180.
5. Park, S.; An, J.; Jung, I.; Piner, R. D.; An, S. J.; Li, X.; Velamakanni, A.; Ruoff, R. S. *Nano Lett.* **2009**, *9*, 1593.
6. Zdrahala, R. J.; Zdrahala, I. J. *J. Biomater. Appl.* **1999**, *14*, 67.
7. Stokes, K.; McVenes, R.; Anderson, J. M. *J. Biomater. Appl.* **1995**, *9*, 321.
8. Christenson, E. M.; Anderson, J. M.; Hiltner, A. *J. Biomed. Mater. Res. Part A* **2004**, *70*, 245.
9. Khan, I.; Smith, N.; Jones, E.; Finch, D. S.; Cameron, R. E. *Biomaterials* **2005**, *26*, 621.

10. Stamatialis, D. F.; Papenburg, B. J.; Gironés, M.; Saiful, S.; Bettahalli, S. N.; Schmitmeier, S.; Wessling, M. *J. Membr. Sci* **2008**, *308*, 1.
11. Jeschke, M. G.; Hermanutz, V.; Wolf, S. E.; Köveker, G. B. *J. Vasc. Surg.* **1999**, *29*, 168.
12. Kim, H.; Miura, Y.; Macosko, C. W. *Chem. Mater.* **2010**, *22*, 3441.
13. Wang, C.; Li, Y.; Ding, G.; Xie, X.; Jiang, M. J. *Appl. Polym. Sci.* **2013**, *127*, 3026.
14. Wan, C.; Chen, B. *Biomed. Mater.* **2011**, *6*, 055010.
15. Marcano, D. C.; Kosynkin, D. V.; Berlin, J. M.; Sinitskii, A.; Sun, Z.; Slesarev, A.; Alemany, L. B.; Lu, W.; Tour, J. M. *ACS Nano* **2010**, *4*, 4806.
16. Xanthos, M. Functional Fillers for Plastics; Wiley: New York: **2010**.
17. Holt, D. S.; Botto, M.; Bygrave, A. E.; Hanna, S. M.; Walport, M. J.; Morgan, B. P. *Blood* **2001**, *98*, 442.
18. Ali, U.; Zhou, Y.; Wang, X.; Lin, T. *J. Text I.* **2012**, *103*, 80.
19. Yang, F.; Murugan, R.; Wang, S.; Ramakrishna, S. *Biomaterials* **2005**, *26*, 2603.
20. Wutticharoenmongkol, P.; Sanchavanakit, N.; Pavasant, P.; Supaphol, P. *Macromol. Biosci.* **2006**, *6*, 70.
21. Coleman, J. N.; Cadek, M.; Blake, R.; Nicolosi, V.; Ryan, K. P.; Belton, C.; Fonseca, A.; Nagy, J. B.; Gun'ko, Y. K.; Blau, W. *J. Adv. Funct. Mater.* **2004**, *14*, 791.
22. Gerschutz, M. J.; Haynes, M. L.; Nixon, D. M.; Colvin, J. M. *J. Rehabil. Res. Dev.* **2011**, *48*, 987.
23. Liu, H.; Brinson, L. C. *Compos. Sci. Technol.* **2008**, *68*, 1502.
24. Yousefi, N.; Gudarzi, M. M.; Zheng, Q.; Lin, X.; Shen, X.; Jia, J.; Sharif, F.; Kim, J.-K. *Compos. A* **2013**, *49*, 42.
25. Jawaid, M.; Abdul Khalil, H.; Alattas, O. S. *Compos. A* **2012**, *43*, 288.
26. Špírková, M.; Pavličević, J.; Strachota, A.; Poreba, R.; Bera, O.; Kaprálková, L.; Baldrian, J.; Šlouf, M.; Lazić, N.; Budinski-Simendić, J. *Eur. Polym. J.* **2011**, *47*, 959.
27. Jacob, M.; Francis, B.; Thomas, S.; Varughese, K. *Polym. Compos.* **2006**, *27*, 671.
28. Spirkova, M.; Poreba, R.; Pavlicevic, J.; Kobera, L.; Baldrian, J.; Pekarek, M. J. *Appl. Polym. Sci.* **2012**, *126*, 1016.
29. Blanton, T.; Majumdar, D.; Melpolder, S. *MRS Symp. Proc.* **2000**, *628*, CC11.
30. Arjun, G.; Ramesh, P. *J. Biomed. Mater. Res. Part A* **2012**, *100*, 3042.
31. Zhao, Y.; Wang, S.; Guo, Q.; Shen, M.; Shi, X. *J. Appl. Polym. Sci.* **2013**, *127*, 4825.